ChemPubSoc Europe

DOI: 10.1002/cmdc.201700429

CHEMMEDCHEM Full Papers

Functional *N*-Formyl Peptide Receptor 2 (FPR2) Antagonists Based on the Ureidopropanamide Scaffold Have Potential To Protect Against Inflammation-Associated Oxidative Stress

Madia L. Stama,[a] Enza Lacivita,*[a] Liliya N. Kirpotina,[b] Mauro Niso,[a] Roberto Perrone,[a] Igor A. Schepetkin,[b] Mark T. Quinn,[b] and Marcello Leopoldo[a]

Formyl peptide receptor 2 (FPR2) is a G protein coupled receptor belonging to the *N*-formyl peptide receptor (FPR) family that plays critical roles in peripheral and brain inflammatory responses. FPR2 has been proposed as a target for the development of drugs that could facilitate the resolution of chronic inflammatory reactions by enhancing endogenous anti-inflammation systems. Starting from lead compounds previously identified in our laboratories, we designed a new series of ureidopropanamide derivatives with the goal of converting functional activity from agonism into antagonism and to develop new FPR2 antagonists. Although none of the compounds behaved as antagonists, some of the compounds were able to induce receptor desensitization and, thus, functionally behaved as antagonists. Evaluation of these compounds in an in vitro model of neuroinflammation showed that they decreased the production of reactive oxygen species in mouse microglial N9 cells after stimulation with lipopolysaccharide. These FPR2 ligands may protect cells from damage due to inflammation-associated oxidative stress.

Introduction

Inflammation is a complex biological response of the body to harmful stimuli, such as infectious agents, tissue damage, and toxins, and involves several immune and inflammatory cells including neutrophils, macrophages, and mast cells. A successful inflammatory response eliminates invading pathogens and is followed by initiation of tissue repair.[1] Similarly, neuroinflammation is a protective mechanism to restore the damaged glial cells and neurons in the central nervous system (CNS). Neuroinflammation is a response that involves all CNS cells, including neurons, microglia, and astrocytes, and is mediated by the inflammatory mediators released from these cells.[2,3] Initially, neuroinflammation is a protective response in the brain that initiates the healing process. However, chronic activation of the immune response can lead to excessive release of pro-inflammatory cytokines and neurotoxic mediators, which can lead to neuronal damage and loss.[2,3] Accumulating evidence suggests that chronic neuroinflammation plays an important role in the onset and progression of several neurodegenerative diseases such as Alzheimer's disease (AD) and Parkinson's disease (PD) as well as in psychiatric disorders.[4,5]

Inflammation is tightly regulated such that pro- and anti-inflammatory mediators operate in a parallel and serial fashion to evoke, at first, the inflammatory response and, then, to ensure resolution of the inflammation.[6] The mechanisms leading to the restoration of homeostasis and resolution of inflammation have been elucidated only recently, and specific pro-resolving mediators, such as lipoxins, resolvins, and maresins, have been identified.[7,8] Among the receptors activated by pro-resolving mediators is the formyl peptide receptor 2 (FPR2), a G protein coupled receptor (GPCR) belonging to the formyl peptide receptor (FPR) family, which also includes the subtypes FPR1 and FPR3.[9] FPRs were first identified in humans[10] and shortly after in other primates[11] and rodents[12] and are expressed in a variety of tissues and cells, including neutrophils, monocytes/macrophages, and microglia. FPR2 are functionally expressed in glial cells and astrocytes.[14,15] Recently, expression of Fpr1 and Fpr2, murine homologues of human FPR, was also reported in rat neuronal stem cells.[17] FPRs play relevant roles in innate immunity, and their stimulation elicits a cascade of host defense reactions, including chemotaxis, superoxide anion ($O_2^{\bullet}$) generation, and exocytosis.[9] FPR2 interacts with a large number of structurally diverse agonists, such as formylated peptides, amyloidogenic peptides, and prion

[a] Dr. M. L. Stama, Prof. E. Lacivita, Dr. M. Niso, Prof. R. Perrone, Prof. M. Leopoldo
Dipartimento di Farmacia—Scienze del Farmaco, Università degli Studi di Bari Aldo Moro, via Orabona, 4, 70125 Bari (Italy)
Fax: (+39) 080-5442231
E-mail: enza.lacivita@uniba.it

[b] Dr. L. N. Kirpotina, Dr. I. A. Schepetkin, Prof. M. T. Quinn
Department of Microbiology and Immunology, Montana State University, Bozeman, MT 59717 (USA)

Supporting Information [synthesis procedures and spectroscopic data for (R)-/(S)-**17**, (R)-/(S)-**18**, (2R)-**30**, (2S)-**32**, (2S)-**33**, (R)-/(S)-**21**, (R)-/(S)-**22**, (2R)-**34**, (2S)-**36**, (2S)-**37**, (R)-/(S)-**23**, (R)-/(S)-**25–27**, (2R)-**38**, (2R)-**39**, (2R)-**46**, (2S)-**40**, (2S)-**41**, (2S)-**47**, (S)-**24**, (2R)-**42**, (2R)-**43**, (2S)-**44**, and (2S)-**45**] and the ORCID identification number(s) for the author(s) of this article can be found under https://doi.org/10.1002/cmdc.201700429.

protein PrP(106–126), which induce pro-inflammatory responses.[9] On the other hand, the N terminus of the calcium-regulated/phospholipid-binding annexin I and the non-peptide agonists lipoxin A_4 (LXA_4) and resolvin D1 exert anti-inflammatory and pro-resolving effects, which suggests a biased signaling capacity of FPR2.[9,17]

The involvement of FPR2 in the resolution of inflammation makes it an attractive target for treating a variety of pathologies characterized by chronic inflammation, such as rheumatoid arthritis, asthma, cystic fibrosis, chronic obstructive pulmonary disease, and CNS diseases.[18,19] For example, it has been reported that in vivo administration of LXA_4 in rats is able to inhibit microglial activation and to diminish neuroinflammation after spinal cord hemisection[20] and hemorrhage.[21] Likewise, the administration of LXA_4[22] or annexin A1[23] in animal models of AD is able to stimulate a pro-resolving activation of microglia by decreasing the levels of pro-inflammatory cytokines, which results in improved β-amyloid clearance and degradation. Finally, it has been suggested that FPRs are involved in the rapid generation of reactive oxygen species (ROS) from enteric commensal bacteria that can function as second messengers in many signal transduction pathways.[24]

To date, several classes of chemically diverse FPR2 agonists have been reported in the literature,[25,26] such as pyrazolone derivatives such as mixed FPR1/FPR2 agonist **1** (designated also as "compound **43**"),[27] *N*-phenylurea derivatives such as compound **2** (also named AG-10/8),[28] and quinazolinones derivatives exemplified by the highly specific FPR2 agonist Quin C1 (compound **3**) (Figure 1).[29] Recently, we developed ureidopropanamide derivatives as agonists of human FPR2, exemplified by compounds (*R*)- and (*S*)-**4** (Figure 1).[30–33] Regarding FPR2 antagonists, several peptide[9] and peptidomimetic antagonists,[34] exemplified by compound **5**, have been reported, whereas only a very limited number of small-molecule antagonists have been described so far (Figure 1). Quinazolinone **6**, also known as Quin C7, was identified through structure–activity relationship analysis of Quin C1. Compound **6** displays a K_i value of 6.7 μM at FPR2 and was characterized as an FPR2 antagonist because it did not activate Ca^{2+} flux in FPR2-transfected cells and inhibited Ca^{2+} flux and chemotaxis induced by the FPR2 agonist WKYMVM. Moreover, compound **6** inhibited arachidonic acid induced ear edema.[35] Another FPR2 antagonist is pyrrolidine bis(diketopiperazine) **7**, which was identified by screening combinatorial libraries, and it is the most potent non-peptidic FPR2 antagonist identified to date (IC_{50} = 81 nM).[36] It is interesting to note that a minor structural change between Quin C1 and Quin C7 (i.e., removal of the methyl group) converted its functional activity from agonism into antagonism. A docking study performed on different classes of FPR2 ligands suggested that the presence of the hydroxy group completely changed the binding mode of Quin C7 relative to that of Quin C1. In particular, Quin C7 lacks interaction with Arg295, which is a critical interaction shared by the majority of FPR2 agonists.[37]

Considering the paucity of small-molecule FPR2 antagonists and the inherent limitations of peptides and peptidomimetics as therapeutic agents, we explored the possibility of developing non-peptide antagonists starting from the ureidopropanamide scaffold. We reasoned that insertion of the hydroxy functionality in the ureidopropanamide scaffold could change the binding mode of the compounds and, therefore, could lead to the interconversion of their functional activity. To this end, we selected compounds (*R*)- and (*S*)-**4** (Table 1) and compound **2** (Table 2), which were previously characterized as FPR2 agonists in our laboratories, as starting points for the development of FPR2 antagonists with ureidopropanamide structures.[28,33]

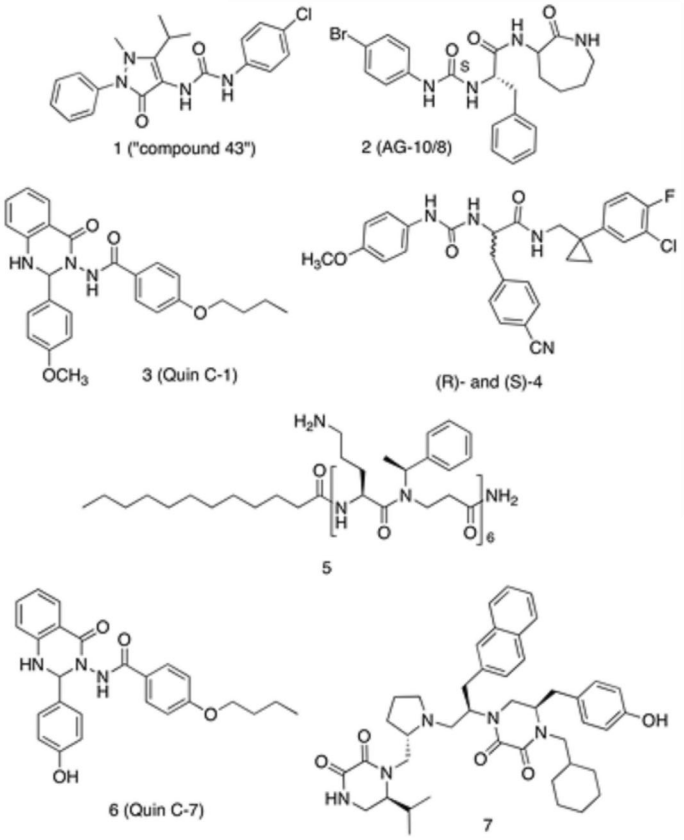

Figure 1. Chemical structures of FPR2 agonists and antagonists.

Results and Discussion

Study design

The aim of this study was to identify new FPR2 antagonists by structural manipulation of the ureidopropanamide scaffold of agonists **2** and **4**. Many examples have been reported in which small structural modifications to GPCR-targeted ligands led to major changes in their functional activity, converting agonists into antagonists or vice versa.[38] An example is the FPR2 antagonist Quin C7, in which the replacement of the methoxy group on the 2-phenyl ring of the quinazolinone backbone in Quin C1 with a hydroxy substituent resulted in the reversal of bioactivity.[39] Therefore, we modified selected ureidopropanamide agonists **2** and **4** by introducing a hydroxy group on each aromatic ring [compounds (*R*)- and (*S*)-**24**–**27**, Table 1;

Table 1. Biological activity of ureidopropanamides derived from modification of compounds (*R*)- and (*S*)-**4**.

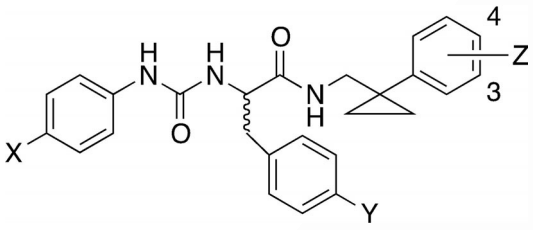

Compd	X	Y	Z	Ca^{+2} mobilization FPR2-HL60 EC_{50} [μM] (efficacy [%])[a]	Ca^{+2} mobilization FPR1-HL60 EC_{50} [μM] (efficacy [%])[a]	Ca^{+2} mobilization FPR2-HL60 IC_{50} [μM] (max. inhib. [%])[a]	Ca^{+2} mobilization FPR1-HL60 IC_{50} [μM] (max. inhib. [%])[a]	MTT EC_{50} [μM][a]
(*R*)-**4**	OCH_3	CN	4-Cl,3-F	0.63 ± 0.2 (100)[33]	1.8 ± 0.3 (60)[33]	N.T.	N.T.	N.T.
(*S*)-**4**	OCH_3	CN	4-Cl,3-F	0.45 ± 0.1 (115)[33]	3.4 ± 0.9 (60)[33]	N.T.	N.T.	N.T.
(*R*)-**24**	OH	CN	H	N.A.	N.A.	N.A.	N.A.	> 100
(*S*)-**24**	OH	CN	H	N.A.	N.A.	N.A.	16.4 ± 3.4 (55)	> 100
(*R*)-**25**	OCH_3	OH	H	0.41 ± 0.16 (90)	5.1 ± 1.3 (55)	24.8 ± 2.4 (75)	N.A.	> 100
(*S*)-**25**	OCH_3	OH	H	2.9 ± 0.8 (130)	1.5 ± 0.3 (95)	9.8 ± 2.1 (95)	N.A.	> 100
(*R*)-**26**	OCH_3	CN	3-OH	2.6 ± 0.14 (65)	N.A.	2.1 ± 0.4 (60)	N.A.	44.4
(*S*)-**26**	OCH_3	CN	3-OH	0.18 ± 0.09 (115)	1.4 ± 0.4 (100)	0.98 ± 0.13 (85)	N.A.	> 100
(*R*)-**27**	OCH_3	CN	4-OH	7.0 ± 2.0 (70)	N.A.	29.5 ± 2.6 (50)	N.A.	> 100
(*S*)-**27**	OCH_3	CN	4-OH	1.6 ± 0.5 (75)	1.3 ± 0.4 (120)	3.7 ± 1.3 (85)	N.A.	21.8

[a] Data are the mean of three independent experiments; N.T. = not tested; N.A. = not active.

Table 2. Biological activity of ureidopropanamides derived from modification of compound **2**.

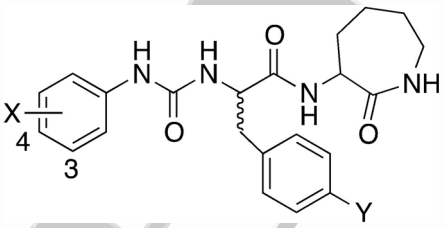

Compd	X	Y	Ca^{+2} mobilization FPR2-HL60 EC_{50} [μM] (efficacy [%])[a]	Ca^{+2} mobilization FPR1-HL60 EC_{50} [μM] (efficacy [%])[a]	Ca^{+2} mobilization FPR2-HL60 IC_{50} [μM] (max. inhib. [%])[a]	Ca^{+2} mobilization FPR1-HL60 IC_{50} [μM] (max. inhib. [%])[a]	MTT EC_{50} [μM][a]
(*S*)-**2**	4-Br	H	0.004 ± 0.002 (115)[28]	0.3 ± 0.08 (135)[28]	N.T.	N.T.	N.T.
(2*R*)-**42**	4-OH	H	N.A.	N.A.	N.A.	N.A.	> 100
(2*R*)-**43**	3-OH	H	N.A.	12.5 ± 2.5 (90)	N.A.	N.A.	> 100
(2*S*)-**44**	4-OH	H	N.A.	11.0 ± 3.6 (65)	N.A.	N.A.	> 100
(2*S*)-**45**	3-OH	H	N.A.	0.55 ± 0.13 (90)	N.A.	1.2 ± 0.4 (90)	> 100
(2*R*)-**46**	4-Br	OH	0.35 ± 0.12 (140)	0.82 ± 0.37 (110)	25.3 ± 7.2 (100)	0.56 ± 0.17 (85)	> 100
(2*S*)-**47**	4-Br	OH	0.78 ± 0.23 (90)	0.23 ± 0.05 (125)	2.1 ± 0.6 (100)	0.076 ± 0.014 (95)	> 100

[a] Data are the mean of three independent experiments; N.T. = not tested; N.A. = not active.

compounds (2*R*)-**42**, (2*R*)-**43**, and (2*R*)-**46** and (2*S*)-**44**, (2*S*)-**45**, and (2*S*)-**47**, Table 2).

Chemistry

The synthesis of target compounds (*R*)- and (*S*)-**24**–**27** is shown in Scheme 1. Amine **10** was prepared according to reported protocols.[39] Amines **13** and **14** were prepared by demethylation of intermediates **11** and **12**,[39] respectively, by using BBr_3/CH_2Cl_2. Amines **10**, **13**, and **14** were then condensed with appropriate (*R*)-*tert*-butoxycarbonyl (Boc)- or (*S*)-Boc-amino acids **8** and **9** after activation with *N*,*N*′-carbonyldiimidazole to obtain Boc-protected derivatives (*R*)- and (*S*)-**15**–**18**. Subsequently, these latter compounds were deprotected with 3 N hydrochloric acid to obtain amines (*R*)- and (*S*)-**19**–**22**. Target compounds (*R*)- and (*S*)-**25**–**27** were obtained by condensing amines (*R*)- and (*S*)-**20**–**21** with the appropriate phenylisocyanate. These compounds were obtained in low yields because of the low solubility of the reagents in the commonly used solvents. Demethylation of compounds (*R*)- and (*S*)-**23**, which were prepared by condensing amines (*R*)- and (*S*)-**19** with 4-methoxyphenylisocyanate, gave target compounds (*R*)- and (*S*)-**24**. Also, in this case, the reaction proceeded with very low yield because of the low solubility of compounds (*R*)- and (*S*)-

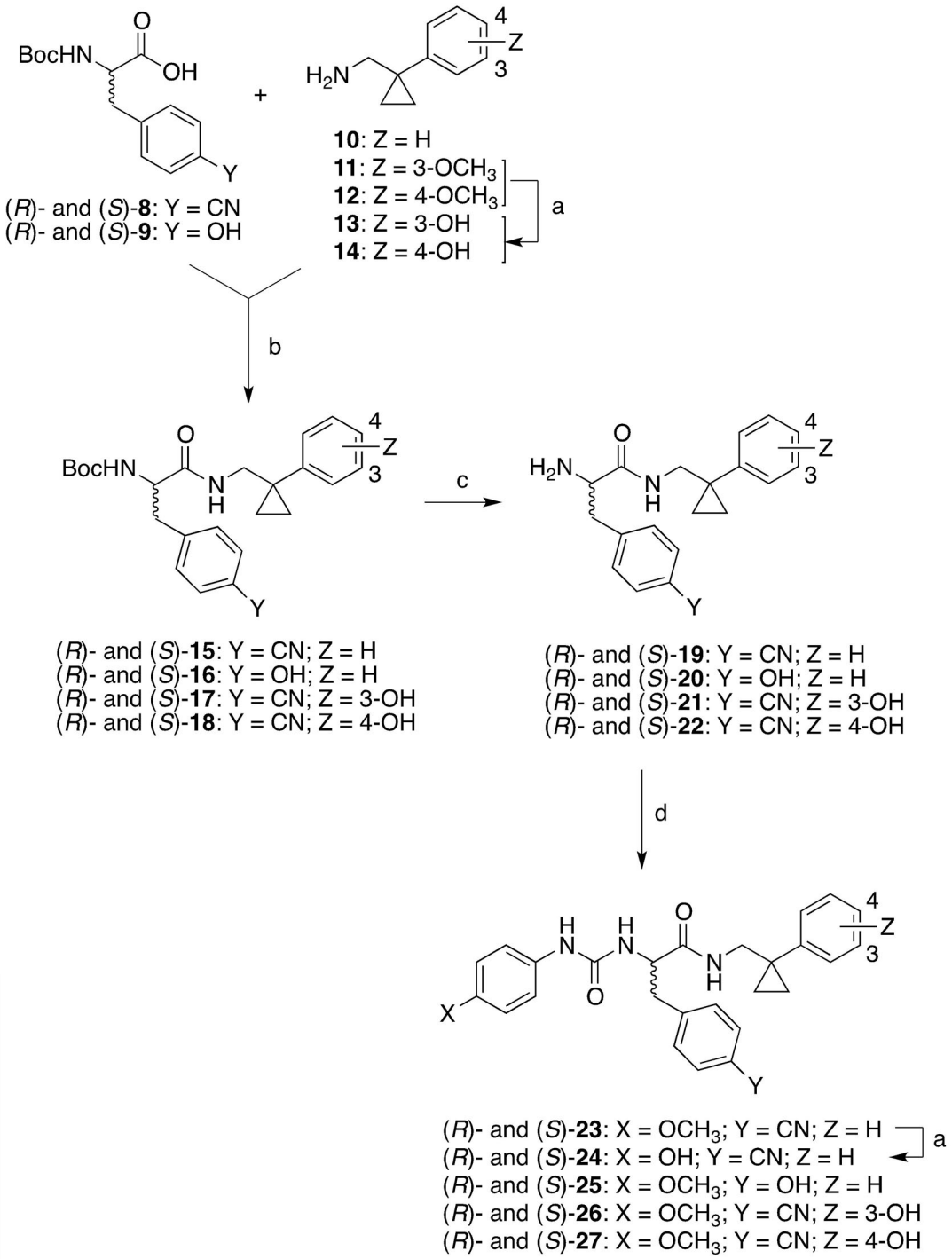

Scheme 1. Synthesis of target compounds (*R*)- and (*S*)-**24**–**27**. *Reagents and conditions*: a) BBr_3, CH_2Cl_2, 0 °C→RT, 4 h; b) *N*,*N*′-carbonyldiimidazole, RT, overnight; c) 3 N HCl, dioxane, RT, 24 h; d) 4-methoxyphenylisocyanate, RT, overnight.

23 in anhydrous CH_2Cl_2. The use of different solvents did not lead to a substantial increase in the yield.

Target compounds (2*R*)-**42**, (2*R*)-**43**, and (2*R*)-**46** and (2*S*)-**44**, (2*S*)-**45**, and (2*S*)-**47**, which are structurally related to compound **2**, were prepared in a similar fashion according to Scheme 2. (*R*)-Boc- and (*S*)-Boc-phenylalanine (**28**) and (*R*)-Boc- or (*S*)-Boc-tyrosine (**9**) were condensed with commercially available 2-amino-ε-caprolactam (**29**) after activation with *N*,*N*′-carbonyldiimidazole to obtain Boc-protected derivatives (2*R*)-**30** and (2*R*)-**31** and (2*S*)-**32** and (2*S*)-**33**. Subsequently, these latter compounds were deprotected with 3 N hydrochloric acid to obtain amines (2*R*)-**34** and (2*R*)-**35** and (2*S*)-**36** and (2*S*)-**37**. Target compounds (2*R*)-**46** and (2*S*)-**47** were obtained by condensing amines (2*R*)-**35** and (2*S*)-**37** with 4-bromophenylisocyanate, respectively. For both compounds, low yields were observed because of the low solubility of the reagents in the

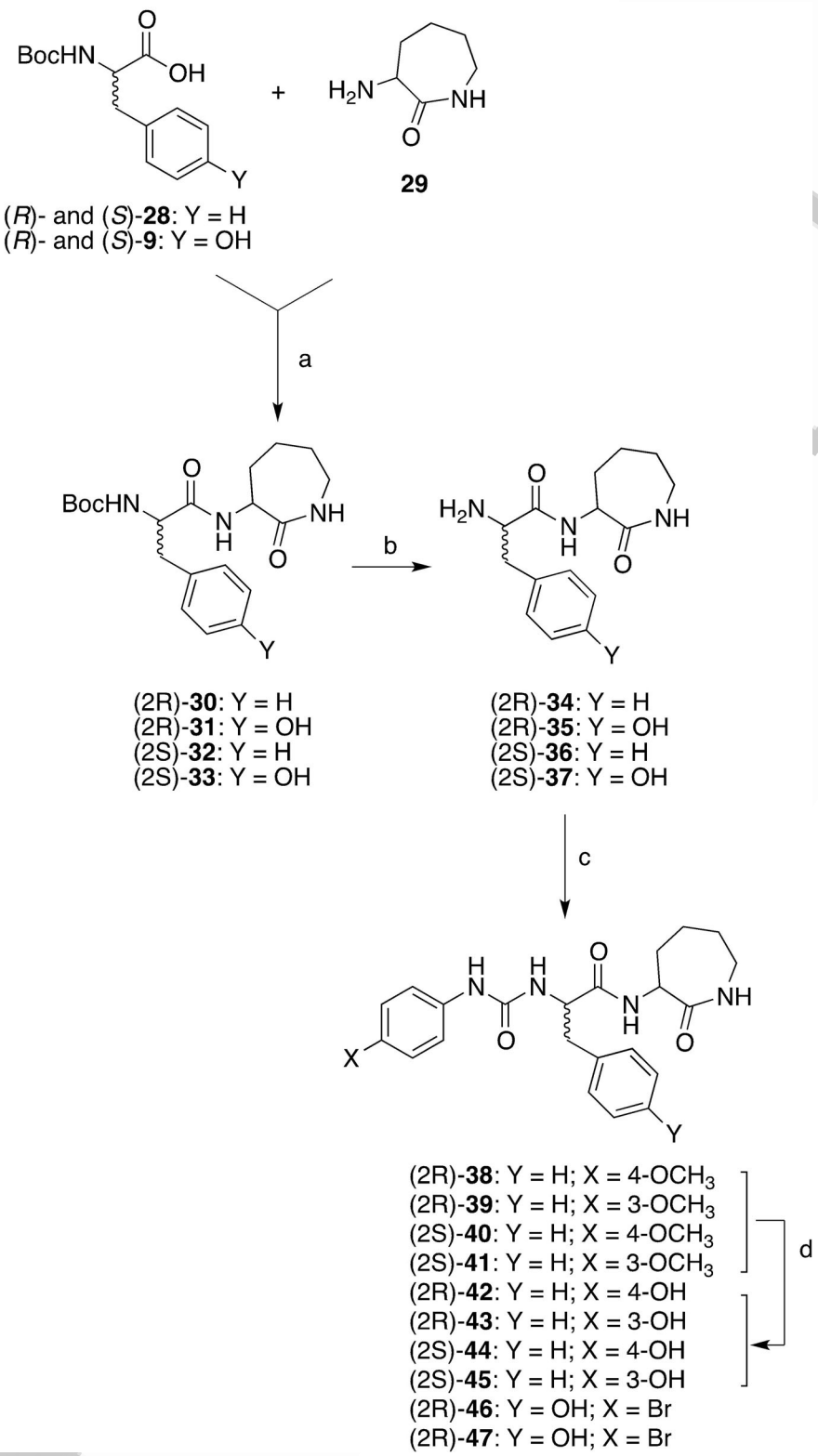

Scheme 2. Synthesis of target compounds (2*R*)-**42**, (2*R*)-**43**, and (2*R*)-**46** and (2*S*)-**44**, (2*S*)-**45**, and (2*S*)-**47**. *Reagents and conditions*: a) *N*,*N*′-carbonyldiimidazole, RT, overnight; b) 3 N HCl, dioxane, RT, 24 h; c) 4-substituted phenylisocyanate, RT, overnight; d) BBr_3, CH_2Cl_2, 0 °C→RT, 4 h.

commonly used solvents, such THF and dioxane. Target compounds (2*R*)-**42** and (2*R*)-**43** and (2*S*)-**44** and (2*S*)-**45** were prepared by demethylation of compounds (2*R*)-**38** and **39** and (2*S*)-**40** and (2*S*)-**41**, which were prepared by condensing amines (2*R*)-**34** and (*S*)-**36** with 4-methoxy- and 3-methoxyphenylisocynate, respectively.

Intrinsic activity of the target compounds

The functional activity of the newly synthesized compounds was assessed in HL-60 cells transfected with human FPR2 by evaluating their effect on intracellular Ca^{2+} flux. The functional activity at FPR1 was also assessed in HL-60 cells transfected with human FPR1 to determine compound selectivity.

The first group of compounds originated from agonists (*R*)- and (*S*)-**4** (Table 1). The data indicate that none of the compounds behaved as FPR2 antagonists and thus suggest that the simple introduction of a hydroxy substituent on one of the aromatic rings of the ureidopropanamide derivatives did not convert the functional response from agonism into antagonism. However, the introduction of the hydroxy group did have different impacts on the biological activity depending on its location. For example, if the hydroxy group was introduced in the 4-position of the phenylureidic moiety [as in compounds (*R*)- and (*S*)-**24**], the compounds did not induce Ca^{2+} mobilization in FPR2-HL60 cells and did not block Ca^{2+} mobilization induced by an agonist in these cells, which indicated that the compounds were no longer able to interact with FPR2.

This result was quite unexpected, because a previous structure–activity study indicated that different substituents, including polar groups such as NO_2 and CN, were well tolerated in that position.[33] Thus, it is likely that the introduction of a hydrogen-bond-donor substituent was not tolerated in this part of the molecule. On the other hand, (*R*)- and (*S*)-**24** behaved as FPR1 antagonists and inhibited Ca^{2+} mobilization induced by *f*MLF.■■Please define *f*MLF?■■

Replacement of the cyano group of compounds (*R*)- and (*S*)-**4** with a hydroxy group was well tolerated. In fact, (*R*)- and (*S*)-**25** exhibited EC_{50} values similar to those of compounds (*R*)- and (*S*)-**4** at both FPR2 and FPR1, and this confirmed our previous findings that a polar group was well tolerated in that position.[30,33] If the hydroxy substituent was introduced on the phenyl ring of the "right-hand side" of the molecule, different effects were observed depending on the position and the chirality of the molecule. Indeed, the *R* enantiomers were less active than their *S* counterparts. In addition, if the hydroxy group was introduced at the 3-position, resulting compound (*S*)-**26** had an EC_{50} value similar to that of compound (*S*)-**4**, whereas the agonist potency of 4-substituted derivative (*S*)-**27** was slightly lower than that of (*S*)-**4**. This trend is in line with our previous findings and suggests that the size and position of the substituent in this part of the molecule influences the interaction with FPR2.[33] Finally, *R* enantiomers **26** and **27** were not able to activate FPR1, whereas the *S* enantiomers had EC_{50} values similar to that of (*S*)-**4**.

Analysis of the derivatives of agonist **2** (Table 2) showed that introduction of a hydroxy substituent on the phenyl group linked to the ureidic group led to a complete loss of FPR2 agonist activity and a substantial decrease in agonist potency for FPR1. This effect was more pronounced if the hydroxy group was placed in the 4-position, and this confirmed that the introduction of a hydrogen-bond-donor substituent in this part of the molecule did not allow a favorable interaction with FPR2. Replacement of the phenylalanine residue in **2** with a tyrosine residue led to a decrease in FPR2 agonist potency [compounds (2*R*)-**46** and (2*S*)-**47**], although the compounds showed EC_{50} values in the low micromolar range. On the other hand, this structural modification did not influence the interaction with FPR1.

Given that none of the compounds behaved as an antagonist, we evaluated if they were able to induce receptor desensitization and, thus, if they could behave functionally as FPR2 antagonists. It is known that after stimulation with *N*-formyl peptides FPRs undergo homologous desensitization, and as a result, the cellular responses rapidly decline in intensity and the cells become refractory to subsequent stimulation with agonists.[9] Desensitization is one of the mechanisms for controlling and regulating GPCR signaling and trafficking,[40] and it has been proposed that targeting desensitization machinery would result in fine-tuning of physiological responses.[41] For example, recent studies demonstrated that LXA_4 stimulation induced FPR2 internalization, which is critical for phagocytosis of apoptotic cells.[42] In addition, we previously reported that compound **2** was able to induce receptor desensitization in human neutrophils.[28] Therefore, we evaluated if our compounds were able to induce FPR2 desensitization by inhibiting Ca^{2+} mobilization induced by the selective FPR2 agonist WKYMVM. Among the compounds generated from compounds (*R*)- and (*S*)-**4**, only compounds (*R*)- and (*S*)-**26** and (*R*)- and (*S*)-**27**, in which the hydroxy group was inserted in the phenyl ring of the "right-hand side" of the molecule, were able to induce FPR2 desensitization with IC_{50} values similar to those of their EC_{50} values. Regarding compounds (2*R*)-**42**, (2*R*)-**43**, and (2*R*)-**46** and (2*S*)-**44**, (2*S*)-**45**, and (2*S*)-**47**, formally derived from compound **2**, only compounds (2*R*)-**46** and (2*S*)-**47** were able to induce desensitization. Compounds (2*S*)-**45**, (2*R*)-**46**, and (2*S*)-**47** were able to induce FPR1 desensitization. Again, their IC_{50} values were found to be similar to their EC_{50} values, with the exception of compound (2*R*)-**46**, which was less effective at desensitizing FPR2. These data suggest that agonist-selective desensitization is related to subtle changes in the molecular structure.

Effect of selected compounds on ROS production in N9 cells

Considering the ability of our FPR2 agonists to induce receptor desensitization, we considered whether they could exert a protective effect in an in vitro model of neuroinflammation. To address this issue, we evaluated their effects in mouse microglia N9 cells, which have been extensively used as a representative model of primary microglial cells.[43] Moreover, it was reported that N9 cells express low levels of FPR2 mRNA under resting conditions, whereas FPR2 mRNA expression is induced in a time-dependent manner upon cell activation by bacterial endotoxin lipopolysaccharide (LPS) or others inflammatory stimulus, such as β-amyloid.[44,45]

Initially, we evaluated the effect of newly synthesized compounds on metabolic activity in N9 cells under resting conditions by using the MTT (3-[4,5-dimethylthiazol-2-yl]-2,5-diphenyltetrazolium bromide) assay, which quantifies mitochondrial activity in living cells, to assess cytotoxicity of the compounds.

The data indicate that none of the compounds, except (*R*)-**26** and (*S*)-**27**, were cytotoxic after 24 h treatment in a concentration range of 0.1 to 100 μM ($EC_{50} > 100$ μM) (Tables 1 and 2).

Next, among the studied compounds, we selected desensitizing compounds (*R*)-**25**, (*R*)- and (*S*)-**26**, (*R*)- and (*S*)-**27**, (2*R*)-**46**, and (2*S*)-**47** to evaluate if they were able to modulate oxidant stress in N9 cells induced by an inflammatory stimulus, that is, 24 h treatment with LPS. In particular, we measured the effects on ROS production, and for comparative purposes, we included also the reference agonist Quin C1, which is also able to induce FPR2 desensitization ($IC_{50} = 0.04$ μM) and displays anti-inflammatory properties in vivo.[29] Under physiological conditions, ROS are involved in immune responses and inflammation, as well as synaptic plasticity, learning, and memory.[46,47] Recently, it was reported that FPR2 promoted neural differentiation in mouse neural stem cells through ROS generation.[48] However, if produced in excess, ROS can induce oxidative stress, damage proteins and DNA, and induce lipid peroxidation. Oxidative stress can trigger cell death and has been implicated in the pathogenesis of many neurodegenerative diseases, including AD.[49]

Assessment of the effect of (*R*)-**25**, (*R*)- and (*S*)-**26**, (*R*)- and (*S*)-**27**, (2*R*)-**46**, and (2*S*)-**47** and Quin C1 in N9 cells after 24 h stimulation with LPS showed that at a 0.1 μM concentration, only Quin C1, (*R*)-**25**, and (2*R*)-**46** induced a statistically significant decrease in ROS production ($p < 0.05$) (Figure 2). Upon testing the compounds at a 1 μM concentration, a statistically significant decrease in ROS production was observed for all of the tested compounds, except for compound (*S*)-**26** ($p < 0.05$) (Figure 2), which is indicative of dose dependence of this response. Moreover, except for compound (*S*)-**26**, the decrease in ROS production correlated with the levels of receptor desensitization measured for the respective compounds.

We also evaluated the direct ROS scavenging activity of (*R*)-**25**, (*R*)- and (*S*)-**26**, (*R*)- and (*S*)-**27**, (2*R*)-**46**, and (2*S*)-**47** by using a non-enzymatic $O_2^{\bullet-}$-generating system (phenazine methosulfate/NADH). Importantly, none of the tested compounds demonstrated ROS scavenging activity at concentrations up to 20 μM (data not shown), which indicated that (*R*)- and (*S*)-**26**, (*R*)- and (*S*)-**27**, (2*R*)-**46**, and (2*S*)-**47** behaved as functional antagonists and not as ROS scavengers and that they were able to exert protective effects in our model of neuroinflammation through receptor desensitization and possibly cross-desensitization.

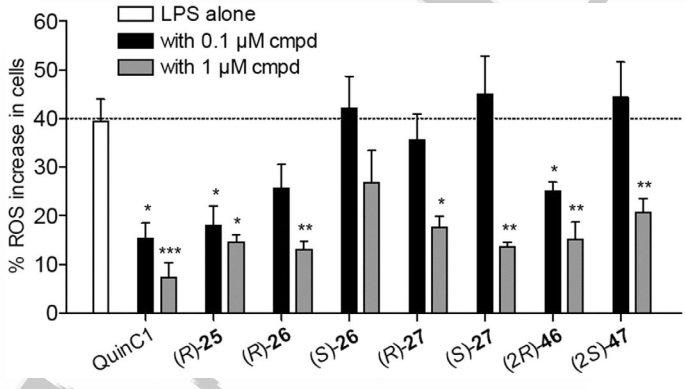

Figure 2. Effect of compounds of selected FPR2 ligands on ROS production in mouse N9 cells. The white bar is the percent increase in ROS observed after 24 h treatment with LPS as compared with control. The black and gray bars are the percent increase in ROS observed after 24 h co-incubation of test compound and LPS at 0.1 and 1 μM, respectively, relative to control ($p < 0.05$).

Conclusions

In summary, we manipulated the structure of the formyl peptide receptor 2 (FPR2) agonists (*R*)- and (*S*)-**4** and **2** to develop FPR2 antagonists with a ureidopropanamide scaffold. We inserted a hydroxy group on each aromatic ring individually in an effort to interconvert functional activity from agonism to antagonism, as the same structural modification on the quinazolinone agonist Quin C1 led to the antagonist Quin C7. We prepared and tested 14 new structurally related ureidopropanamide derivatives. Although none of the compounds behaved as an antagonist, some of the compounds were able to induce receptor desensitization, and they thus behaved as functional antagonists. Further analysis of compounds (*R*)-**25**, (*R*)- and (*S*)-**26**, (*R*)- and (*S*)-**27**, (2*R*)-**46**, and (2*S*)-**47** in an in vitro model of neuroinflammation showed that these compounds did not induce an inflammatory response in unstimulated mouse microglial N9 cells but were able to significantly decrease the production of reactive oxygen species (ROS) if the cells were stimulated with lipopolysaccharide, thereby exerting protective effects against oxidative stress. In particular, (*R*)-3-(4-hydroxyphenyl)-2-[3-(4-methoxyphenyl)ureido]-*N*-[(1-phenylcyclopropyl)methyl]propanamide [(*R*)-**25**] and (2*R*)-2-[3-(4-bromophenyl)ureido]-3-(4-hydroxyphenyl)-*N*-(2-oxoazepan-3-yl)propanamide [(2*R*)-**46**] induced a dose-dependent decrease in cellular ROS levels. These data are very promising, because oxidative stress is implicated in the pathogenesis of many neurodegenerative diseases, and this opens new questions if other FPR2 agonists capable of desensitizing the receptor can exert protective effect against inflammation-associated oxidative stress. Future studies will assess if these compounds can also exert anti-inflammatory effects by decreasing the intracellular levels of pro-inflammatory mediators through the desensitization of FPR2.

Experimental Section

General procedures

Chemicals were purchased from Sigma–Aldrich, Alfa Aesar, and TCI Chemicals. Unless otherwise stated, all chemicals were used without further purification. Thin-layer chromatography (TLC) was performed by using plates from Merck (silica gel 60 F254). Column chromatography was performed with 1:30 Merck silica gel 60 Å (63–200 μm) as the stationary phase. Flash chromatographic separations were performed with a Biotage SP1 purification system by using flash cartridges prepacked with KP-Sil 32–63 μm, 60 Å silica gel. ^{1}H NMR spectra were recorded with a Varian Mercury-VX spectrometer (300 MHz) or an Agilent NMR spectrometer (500 MHz). All chemical shift values are reported in ppm (δ). For enantiomeric

pairs, NMR spectra of both enantiomers were recorded; however, only the NMR spectrum of the *R* enantiomer is reported in the Experimental Section. Recording of mass spectra was performed with an HP6890-5973 MSD gas chromatograph/mass spectrometer; only significant *m/z* signals, with their percentage of relative intensity in parentheses, are reported. HRMS (ESI) analyses were performed with a Bruker Daltonics MicrOTOF-Q II mass spectrometer, in the mass range of $m/z = 50$ to 800, with an electrospray ion source in the positive- or negative-ion mode. All spectra were in accordance with the assigned structures. The purities of the target compounds listed in Tables 1 and 2 were assessed by reversed-phase (RP)-HPLC and combustion analysis. All compounds showed ≥98% purity. RP-HPLC analysis was performed with an Agilent 1260 Infinity Binary LC System equipped with a diode array detector by using a Phenomenex Gemini C_{18} column (250×4.6 mm, 5 μm particle size). All target compounds were eluted with CH_3OH/H_2O (8:2 *v/v*) at a flow rate of 1 mL min^{-1}. Elemental analyses (C,H,N) of the target compounds were performed with an Eurovector Euro EA 3000 analyzer. Analyses indicated by the symbols of the elements were within ±0.4% of the theoretical values. Enantiomeric purity of target compounds (*R*)- and (*S*)-**24**–**27** was assessed by chiral-phase HPLC analysis with a PerkinElmer series 200 LC instrument by using a Daicel ChiralCel OD column (250 mm×4.6 mm, 5 μm particle size) and equipped with a PerkinElmer 785A UV/Vis detector setting $\lambda = 230$ nm. The compounds were eluted with *n*-hexane/EtOH (4:1 *v/v*) at a flow rate of 0.8 mL min^{-1}. All compounds showed enantiomeric excesses ≥98%.

The following compounds were prepared as previously described: [1-(phenyl)cyclopropyl]methanamine (**10**),[39] [1-(3-methoxyphenyl)-cyclopropyl]methanamine (**11**),[39] [1-(4-methoxyphenyl)cyclopropyl]methanamine (**12**),[39] (*R*)- and (*S*)-*tert*-butyl [3-(4-cyanophenyl)-1-({[1-(phenyl)cyclopropyl]methyl}amino)-1-oxopropan-2-yl]carbamate [(*R*)- and (*S*)-**15**],[33] (*R*)- and (*S*)-2-amino-3-(4-cyanophenyl)-*N*-[(1-phenylcyclopropyl)methyl]propanamide [(*R*)- and (*S*)-**19**].[33]

Synthesis

General procedure for the synthesis of Boc-protected derivatives (*R*)- and (*S*)-16 and (2*R*)-31: *N*,*N*′-Carbonyldiimidazole (1.1 mmol) was added to a solution of (*R*)- or (*S*)-Boc-protected amino acid (1.0 mmol) in anhydrous THF (10 mL) under a N_2 atmosphere. The mixture was stirred at room temperature overnight, and then a solution of the appropriate amine (1.0 mmol) in anhydrous THF (■■volume?■■) was added. The mixture was stirred at room temperature for 6 h. After removal of the solvent in vacuo, the residue was partitioned between EtOAc (20 mL) and H_2O (2× 20 mL). The aqueous layer was separated and extracted with EtOAc (2×20 mL). The collected organic layer was dried (Na_2SO_4) and concentrated in vacuo. The crude residue was chromatographed to give the pure target compound as a white solid.

(*R*)-*tert*-Butyl [3-(4-hydroxyphenyl)-1-oxo-1-{[(1-phenylcyclopropyl)methyl]amino}propan-2-yl]carbamate [(*R*)-16]: Eluted with $CHCl_3$/EtOAc = 8:2; yield: 40%; ^{1}H NMR (500 MHz, CD_3OD): δ = 0.76–0.88 (m, 4H), 1.37 (s, 9H), 2.63 (dd, J = 13.7, 8.3 Hz, 1H), 2.75 (dd, J = 13.7, 8.3 Hz, 1H), 2.85 (dd, J = 13.7, 5.9 Hz, 1H), 2.95 (dd, J = 13.7, 5.9 Hz, 1H), 4.13–4.17 (m, 1H), 6.68 (d, J = 8.3 Hz, 2H), 6.74 (brd, 1H), 6.96–6.99 (m, 2H), 7.18 (brt, 1H), 7.23–7.30 ppm (m, 5H); MS (ESI$^+$): m/z = 433 [M + Na]$^+$; MS–MS (ESI$^+$): m/z (%) = 333 (100).

(*S*)-*tert*-Butyl [3-(4-Hydroxyphenyl)-1-oxo-1-{[(1-phenylcyclopropyl)methyl]amino}propan-2-yl]carbamate [(*S*)-16]: Eluted with $CHCl_3$/EtOAc = 8:2; yield: 30%; MS (ESI$^+$): m/z = 433 [M + Na]$^+$; MS–MS (ESI$^+$): m/z (%) = 333 (100).

(2*R*)-*tert*-Butyl {3-(4-hydroxyphenyl)-1-oxo-1-[(2-oxoazepan-3-yl)amino]propan-2-yl}carbamate [(2*R*)-31]: Eluted with $CHCl_3$/MeOH = 19:1; yield: 60%; ^{1}H NMR (500 MHz, $CDCl_3$): δ = 1.23–1.49 (m + s, 11H), 1.76–1.81 (m, 3H, 1H D_2O exchanged), 1.89–2.07 (m, 2H), 2.92–3.00 (m, 2H), 3.22–3.26 (m, 2H), 4.36–4.46 (m, 2H), 5.14–5.30 (m, 1H), 6.39–6.47 (m, 1H), 6.72–6.74 (m, 2H), 6.85–7.05 (m, 2H), 7.12 ppm (brs, 1H). MS (ESI$^+$): m/z = 414 [M + Na]$^+$, MS–MS (ESI$^+$): m/z (%) = 314 (100).

General procedure for the synthesis of amines (*R*)- and (*S*)-20 and (2*S*)-35: To a solution of Boc-protected derivative (*R*)- and (*S*)-**16** or (2*R*)-**31** (0.46 mmol) in 1,4-dioxane (10 mL) was added 3 N hydrochloric acid (5 mL). The mixture was stirred at room temperature for 24 h and basified with 5% aq NaOH.■■Please give approx. pH value?■■ The separated aqueous phase was extracted with EtOAc (2×20 mL). The combined organic layer was dried (Na_2SO_4) and concentrated in vacuo to afford the pure target amine (quantitative yield) as a colorless oil.

(*R*)-2-Amino-3-(4-hydroxyphenyl)-*N*-[(1-phenylcyclopropyl)methyl]propanamide [(*R*)-20]: ^{1}H NMR (500 MHz, CD_3OD): δ = 0.77–0.87 (m, 4H), 2.62 (dd, J = 13.7, 6.8 Hz, 1H), 2.80 (dd, J = 13.7, 6.4 Hz, 1H), 3.30–3.35 (m, 2H), 3.40–3.45 (m, 2H), 6.71 (d, J = 8.3 Hz, 2H), 6.97 (d, J = 8.3 Hz, 2H), 7.16 (brt, 1H), 7.15–7.19 (brt, 1H), 7.23–7.30 ppm (m, 5H); MS (ESI$^+$): m/z = 333 [M + Na]$^+$; MS–MS (ESI$^+$): m/z (%) = 162 (100), 131 (64).

(*S*)-2-Amino-3-(4-hydroxyphenyl)-*N*-[(1-phenylcyclopropyl)methyl]propanamide [(*S*)-20]: MS (ESI$^+$): m/z = 333 [M + Na]$^+$; MS–MS (ESI$^+$): m/z (%) = 162 (100), 131 (62).

(2*R*)-2-Amino-3-(4-hydroxyphenyl)-*N*-(2-oxoazepan-3-yl)propanamide [(2*R*)-35]: ^{1}H NMR (500 MHz, CD_3OD): δ = 1.22–1.57 (m, 2H), 1.66–2.05 (m, 4H), 1.98–2.02 (m, 2H), 2.87–3.09 (m, 1H), 3.19–3.30 (m, 3H), 3.51–3.77 (m, 1H), 4.47–4.58 (m, 1H), 6.76 (d, J = 8.3 Hz, 2H), 7.02–7.16 ppm (m, 2H); MS (ESI$^-$): m/z = 314 [M + Na]$^+$; MS–MS (ESI$^+$): m/z (%) = 84 (100), 120 (49).

General procedure for the synthesis of (*R*)-23, (*R*)-25, and (2*R*)-46: To a solution of amine (*R*)- or (*S*)-**19**, (*R*)- or (*S*)-**20**, or (2*R*)-**35** (1.0 mmol) in anhydrous THF (■■volume?■■) was added a solution of the appropriate 4-substituted phenylisocyanate (1.2 mmol) in the same solvent (10 mL), and the mixture was stirred at room temperature overnight. After removing the solvent in vacuo, the residue was dissolved in $CHCl_3$ (20 mL) and washed with H_2O (2× 20 mL). The separated organic layer was dried with Na_2SO_4 and concentrated under reduced pressure. The crude residue was purified by chromatography. If necessary, the obtained solid was further purified by crystallization (MeOH) to give the pure target compound.

(*R*)-3-(4-Cyanophenyl)-2-[3-(4-methoxyphenyl)ureido]-*N*-[(1-phenylcyclopropyl)methyl]propanamide [(*R*)-23]: Eluted with $CHCl_3$/EtOAc = 8:2; yield: 47%; ^{1}H NMR (500 MHz, [D_6]DMSO): δ = 0.69–0.71 (m, 1H), 0.77–0.79 (m, 1H), 0.82–0.85 (m, 2H), 2.76 (dd, J = 13.2, 7.8 Hz, 1H), 2.92 (dd, J = 13.7, 4.9 Hz, 1H), 3.18 (dd, J = 13.7, 4.9 Hz, 1H), 3.47 (dd, J = 13.7, 6.4 Hz, 1H), 3.67 (s, 3H), 4.51 (dd, J = 13.2, 7.8 Hz, 1H), 6.20 (d, J = 8.3 Hz, 1H), 6.78 (d, J = 8.8 Hz, 2H), 7.14–7.16 (m, 1H), 7.19–7.26 (m, 8H), 7.67 (d, J = 8.8 Hz, 2H), 8.15 (brt, 1H), 8.42 ppm (s, 1H); MS (ESI$^+$): m/z = 491 [M + Na]$^+$; MS–MS (ESI$^+$): m/z (%) = 491 (100), 342 (20).

(*R*)-3-(4-Hydroxyphenyl)-2-[3-(4-methoxyphenyl)ureido]-*N*-[(1-phenylcyclopropyl)methyl]propanamide [(*R*)-25]: Eluted with

$CHCl_3$/MeOH = 19:1; yield: 17%; ^{1}H NMR (500 MHZ, $CDCl_3$): δ = 0.74–0.79 (m, 4H), 1.71 (brs, 1H, D_2O exchanged), 2.80–2.87 (m, 2H), 3.24 (dd, J = 13.7, 4.4 Hz, 1H), 3.41 (dd, J = 13.7, 5.9 Hz, 1H), 3.72 (s, 3H), 4.46–4.50 (m, 1H), 5.95 (brs, 1H), 6.51 (brt, 1H), 6.62 (d, J = 7.8 Hz, 2H), 6.73 (d, J = 8.3 Hz, 2H), 6.87 (d, J = 8.3 Hz, 2H), 7.02 (d, J = 7.8 Hz, 2H), 7.12–7.16 (m, 4H), 7.20–7.23 ppm (m, 2H); MS (ESI$^+$): m/z = 482 $[M+Na]^+$; MS–MS (ESI$^+$): m/z (%) = 482 (100), 333 (92); elemental analysis calcd (%) for $C_{27}H_{29}N_3O_4$ (459.54): C 70.57, H 6.36, N 9.14, found: C 70.53, H 6.53, N 9.04.

(2*R*)-2-[3-(4-Bromophenyl)ureido]-3-(4-hydroxyphenyl)-*N*-(2-oxooazepan-3-yl)propanamide [(2*R*)-46]: Eluted with $CHCl_3$/MeOH = 98:2; yield: 22%; ^{1}H NMR (500 MHz, [D$_6$]DMSO): δ = 1.16–1.20 (m, 1H), 1.27–1.39 (m, 1H), 1.59–1.87 (m, 4H), 2.67–2.74 (m, 1H), 2.81–2.93 (m, 1H), 3.01–3.05 (m, 1H), 3.11–3.20 (m, 1H), 4.33–4.39 (m, 1H), 4.40–4.47 (m, 1H), 6.28–6.36 (m, 1H), 6.61 (d, J = 8.3 Hz, 2H), 7.00 (dd, J = 8.8, 3.4 Hz, 2H), 7.29 (dd, J = 8.8, 1.5 Hz, 2H), 7.34 (d, J = 8.8 Hz, 2H), 7.81 (brs, 1H), 7.92–8.01 (m, 1H), 8.84 (brd, 1H), 9.14 ppm (s, 1H); MS (ESI$^+$): m/z = 511 $[M+Na]^+$; MS–MS (ESI$^+$): m/z (%) = 340 (22), 314 (100); elemental analysis calcd (%) for $C_{22}H_{25}BrN_4O_4$ (489.36): C 54.00, H 5.15, N 11.46, found: C 54.14, H 5.24, N 11.34.

(*R*)-3-(4-Cyanophenyl)-2-[3-(4-hydroxyphenyl)ureido]-*N*-[(1-phenylcyclopropyl)methyl]propanamide [(*R*)-24]: To a cooled solution of methoxy derivative (*R*)-**23** (2.0 mmol) in anhydrous CH_2Cl_2 (10 mL) was dropwise added 1.0 M boron tribromide in CH_2Cl_2 (3.45 mL, 3.45 mmol). The mixture was stirred at room temperature for 4 h and basified with 10% aq NH_4OH (■■pH value?■■). The separated aqueous phase was extracted with CH_2Cl_2 (2×20 mL). The combined organic layer was dried (Na_2SO_4) and concentrated under reduced pressure. The crude residue was purified by chromatography ($CHCl_3$/MeOH = 98:2) to give the target compound as a solid (5% yield): ^{1}H NMR (500 MHz, [D$_6$]DMSO): δ = 0.69–0.71 (m, 1H), 0.76–0.79 (m, 1H), 0.81–0.84 (m, 2H), 2.76 (dd, J = 13.2, 7.8 Hz, 1H), 2.92 (dd, J = 13.7, 4.9 Hz, 1H), 3.18 (dd, J = 14.2, 4.9 Hz, 1H), 3.47 (dd, J = 13.7, 6.4 Hz, 1H), 4.48–4.52 (m, 1H), 6.14 (d, J = 8.3 Hz, 1H), 6.60 (d, J = 8.8 Hz, 2H), 7.07 (d, J = 8.3 Hz, 2H), 7.11–7.17 (m, 1H), 7.22–7.25 (m, 6H), 7.67 (d, J = 7.8 Hz, 2H), 8.13–8.15 (m, 1H), 8.27 (s, 1H), 8.93 ppm (s, 1H); MS (ESI$^+$): m/z = 477 $[M+Na]^+$; MS–MS (ESI$^+$): m/z (%) = 477 (100), 342 (10). elemental analysis calcd (%) for $C_{27}H_{26}N_4O_3$ (454.52): C 71.35, H 5.77, N 12.33, found: C 71.52, H 5.74, N 12.34.

Biological methods

Materials: Black, 96-well, clear-bottom plates were purchased from PerkinElmer Life and Analytical Sciences (Boston, MA, USA). Cell culture reagents were purchased from EuroClone (Milan, Italy). LPS (lipopolysaccharide from *Escherichia coli* O111:B4), MTT, H_2DCF-DA (2′,7′-dichlorofluorescein diacetate), and Iscove's Modified Dulbecco's Medium were obtained from Sigma–Aldrich (Milan, Italy). Phenazine methosulfate, NADH, and nitro blue tetrazolium (NBT) were purchased from Sigma Chemical Co. (St. Louis, MO, USA).

Cell culture: Human promyelocytic leukemia HL-60 cells stably transfected with FPR1 (FPR1-HL-60 cells) or FPR2 (FPR2-HL-60 cells) (kind gifts from Dr. Marie-Josephe Rabiet, INSERM, Grenoble, France) were cultured in RPMI 1640 medium supplemented with 10% heat-inactivated fetal calf serum, 10 mM HEPES [■■4-(2-hydroxyethyl)-1-piperazineethanesulfonic acid■■], 100 μg mL^{-1} streptomycin, 100 U mL^{-1} penicillin, and G418 (1 mg mL^{-1}), as described previously.[30] Wildtype HL-60 cells were cultured under the same conditions, but without G418.

Murine N9 microglia cells were purchased from Neuro-Zone, Bresso, Italy. N9 cells were grown in Iscove's Modified Dulbecco's Medium supplemented with 5% fetal bovine serum, 2 mM glutamine, 100 U mL^{-1} penicillin, and 100 mg mL^{-1} streptomycin in a humidified incubator at 37 °C under a 5% CO_2 atmosphere.

Ca^{2+} mobilization assay: Changes in intracellular Ca^{2+} in HL-60 cells were measured with a FlexStation 3 scanning fluorimeter (Molecular Devices, Sunnyvale, CA, USA), as described previously.[30] All active compounds were evaluated in parent (wildtype) HL-60 cells to verify that the agonists were inactive in non-transfected cells (not shown). HL-60 cells were suspended in $HBSS^-$ containing 10 mM HEPES, loaded with Fluo-4 AM dye (Invitrogen, Carlsbad, CA, USA) (1.25 μg mL^{-1} final concentration), and incubated for 30 min in the dark at 37 °C. After dye loading, the cells were washed with $HBSS^-$ containing 10 mM HEPES, resuspended in HBSS containing 10 mM HEPES and Ca^{2+} and Mg^{2+} ($HBSS^+$), and aliquoted into the wells of flat-bottomed, half-area-well black microtiter plates (2×10^5 cells per well). The compounds of interest were automatically added from a source plate containing dilutions of test compounds in $HBSS^+$, and changes in fluorescence were monitored (λ_{ex} = 485 nm, λ_{em} = 538 nm) every 5 s for 240 s at room temperature. In desensitization experiments, the dye-loaded cells were pretreated with vehicle (DMSO) or different concentrations of the test compounds, and Ca^{2+} mobilization was monitored. The same wells were then treated with *f*MLF (5 nM) for FPR1-HL-60 cells or WKYMVM (5 nM) for FPR2-HL-60 cells, and Ca^{2+} mobilization was monitored after this second treatment to evaluate desensitization of the response to control peptides. The maximum change in fluorescence, expressed in arbitrary units over baseline, was used to determine agonist response. Responses were normalized to the response induced by 5 nM *f*MLF for FPR1-HL-60 cells or 5 nM WKYMVM for FPR2-HL-60 cells, which were assigned a value of 100%. Each compound was tested in triplicate. Curve fitting (5–6 points) and calculation of median effective concentration values (EC_{50}) were performed by nonlinear regression analysis of the dose–response curves generated by using Prism 5 (GraphPad Software Inc., San Diego, CA, USA).

Cytotoxicity assay: Compound cytotoxicity in N9 cells was determined by evaluating effects on cell growth by using the MTT assay at 24 h.[50,51] On day 1, 20000 cells per well were seeded into 96-well plates at a final volume of 100 μL. On day 2, various concentrations of the test compounds were added (0.1–100 mM). The potential cytotoxic effect of DMSO, which was used to solubilize the test compounds, was also evaluated. After 24 h incubation with the compounds, MTT (0.5 mg mL^{-1}) was added to each well. The plates were incubated at 37 °C for 3–4 h and then the supernatant was removed. The formazan crystals were solubilized in DMSO/EtOH (1:1, 100 mL), and the absorbance values at λ = 570 and 630 nm were measured with a Victor 3 microplate reader (PerkinElmer Life Sciences). EC_{50} values were determined by fitting the absorbance increase percentage versus log[concentration]. Each compound was tested in triplicate at five or six concentrations (10^{-8} to 10^{-4} M). Nonlinear curve fitting was performed by using Prism 6.03 (GraphPad Software Inc., San Diego, CA, USA).

ROS assay: Evaluation of the effect of test compounds on ROS in N9 cells was performed as described by Hornick et al. with minor modifications.[52] A total of 25000 cells per well was seeded into black, 96-well, clear-bottom plates in 100 μL medium. After 3–4 h, LPS (300 ng mL^{-1}), alone or in combination with the test compounds (0.1 or 1 μM), was added to the cells. The plates were incubated at 37 °C for 24 h. H_2DCF-DA was added in 100 μL of medium to yield a final concentration of 10 μM, and the plates were incu-

bated for an additional 30 min. The wells were washed with ice-cold PBS (3×), saline was added, and the fluorescence signals were read with a Tecan Infinity M1000 plate reader by using excitation and emission wavelengths of $\lambda = 480$ and 520 nm, respectively. The increase in fluorescence with respect to the basal level was measured. Statistical analyses and data plotting were performed by using Prism 6.03 (GraphPad Software Inc., San Diego, CA, USA). Results are expressed as mean ± standard error of at least three biological replicates. Differences in ROS production were analyzed by using one-way ANOVA to identify differences and were confirmed with paired two-tailed t-tests. A p value < 0.05 was considered significant.

Evaluation of ROS scavenging activity in cell-free non-enzymatic system: $O_2^{\bullet-}$ was generated by using a nonenzymatic system in the presence or absence of test compounds, and $O_2^{\bullet-}$ was detected by monitoring reduction in NBT to monoformazan dye at $\lambda = 560$ nm, as described previously.[53] The $O_2^{\bullet-}$-generating system contained 3 mM phenazine methosulfate, 200 mM NADH, and 50 mM NBT in 0.05 M phosphate buffer (pH 7.5). The reactions were monitored at $\lambda = 560$ nm with a SpectraMax Plus microplate spectrophotometer at 25 °C, and the rate of absorption change was determined.

Acknowledgements

This research was supported in part by the US National Institutes of Health IDeA Program COBRE Grant GM110732, the USDA National Institute of Food and Agriculture Hatch project 1009546, the Montana University System Research Initiative: 51040-MUSRI2015-03, and the Montana State University Agricultural Experiment Station.

Conflict of interest

The authors declare no conflict of interest.

Keywords: antagonists · inflammation · oxidative stress · receptors · ureidopropanamide

[1] O. P. Kulkarni, J. Lichtnekert, H.-J. Anders, S. R. Mulay, *Mediators Inflamm.* **2016**, 2856213.
[2] T. Shabab, R. Khanabdali, S. Z. Moghadamtousi, H. A. Kadir, G. Mohan, *Int. J. Neurosci.* **2017**, *127*, 624–633.
[3] R. M. Ransohoff, *Science* **2016**, *353*, 777–783.
[4] W. W. Chen, X. Zhang, W. J. Huang, *Mol. Med. Rep.* **2016**, *13*, 3391–3396.
[5] H. Hong, B. S. Kim, H. I. Im, *Int. Neurourol. J.* **2016**, *20*, S2–7.
[6] C. N. Serhan, S. D. Brain, C. D. Buckley, D. W. Gilroy, C. Haslett, L. A. O'Neill, M. Perretti, A. G. Rossi, J. L. Wallace, *FASEB J.* **2007**, *21*, 325–332.
[7] C. N. Serhan, S. Hong, K. Gronert, S. P. Colgan, P. R. Devchand, G. Mirick, R. L. Moussignac, *J. Exp. Med.* **2002**, *196*, 1025–1037.
[8] C. N. Serhan, S. Krishnamoorthy, A. Recchiuti, N. Chiang, *Curr. Top. Med. Chem.* **2011**, *11*, 629–647.
[9] R. D. Ye, F. Boulay, J. M. Wang, C. Dahlgren, C. Gerard, M. Parmentier, C. N. Serhan, P. M. Murphy, *Pharmacol. Rev.* **2009**, *61*, 119–161.
[10] F. Boulay, M. Tardif, L. Brouchon, P. Vignais, *Biochemistry* **1990**, *29*, 11123–11133.
[11] V. Alvarez, E. Coto, F. Setien, S. Gonzalez-Roces, C. Lopez-Larrea, *Immunogenetics* **1996**, *44*, 446–452.
[12] J. L. Gao, P. M. Murphy, *J. Biol. Chem.* **1993**, *268*, 25395–25401.
[13] M. Lacy, J. Jones, S. R. Whittemore, D. L. Haviland, R. A. Wetsel, S. R. Barnum, *J. Neuroimmunol.* **1995**, *61*, 71–78.■■please check–this ref does not appear to be cited within the text.■■
[14] Y. Cui, Y. Le, H. Yazawa, W. Gong, J. M. Wang, *J. Leukoc. Biol.* **2002**, *72*, 628–635.
[15] C. I. Svensson, M. Zattoni, C. N. Serhan, *J. Exp. Med.* **2007**, *204*, 245–252.
[16] G. Wang, L. Zhang, X. Chen, X. Xue, Q. Guo, M. Liu, J. Zhao, *Sci. Rep.* **2016**, *6*, 25946.■■please check–this ref does not appear to be cited within the text.■■
[17] S. Fiore, J. F. Maddox, H. D. Perez, C. N. Serhan, *J. Exp. Med.* **1994**, *180*, 253–260.
[18] M. Perretti, X. Leroy, E. J. Bland, T. Montero-Melendez, *Trends Pharmacol. Sci.* **2015**, *36*, 737–755.
[19] M. Romano, E. Cianci, F. Simiele, A. Recchiuti, *Eur. J. Pharmacol.* **2015**, *760*, 49–63.
[20] A. C. Martini, T. Berta, S. Forner, G. Chen, A. F. Bento, R. R. Ji, G. A. Rae, *J. Neuroinflammation* **2016**, *13*, 75.
[21] Z. Guo, Q. Hu, L. Xu, Z. N. Guo, Y. Ou, Y. He, C. Yin, X. Sun, J. Tang, J. H. Zhang, *Stroke* **2016**, *47*, 490–497.
[22] R. Medeiros, M. Kitazawa, G. F. Passos, D. Baglietto-Vargas, D. Cheng, D. H. Cribbs, F. M. LaFerla, *Am. J. Pathol.* **2013**, *182*, 1780–1789.
[23] M. Ries, R. Loiola, U. N. Shah, S. M. Gentleman, E. Solito, M. Sastre, *J. Neuroinflammation* **2016**, *13*, 234.
[24] R. M. Jones, A. S. Neish, *Free Radical Biol. Med.* **2017**, *105*, 41–47.
[25] I. A. Schepetkin, A. I. Khlebnikov, M. P. Giovannoni, L. N. Kirpotina, A. Cilibrizzi, M. T. Quinn, *Curr. Med. Chem.* **2014**, *21*, 1478–1504.
[26] O. Corminboeuf, X. Leroy, *J. Med. Chem.* **2015**, *58*, 537–559.
[27] R. W. Bürli, H. Xu, X. Zou, K. Muller, J. Golden, M. Frohn, M. Adlam, M. H. Plant, M. Wong, M. McElvain, K. Regal, V. N. Viswanadhan, P. Tagari, R. Hungate, *Bioorg. Med. Chem. Lett.* **2006**, *16*, 3713–3718.
[28] I. A. Schepetkin, L. N. Kirpotina, A. I. Khlebnikov, M. A. Jutila, M. T. Quinn, *Mol. Pharmacol.* **2011**, *79*, 77–90.
[29] M. He, N. Cheng, W. W. Gao, M. Zhang, Y. Y. Zhang, R. D. Ye, M. W. Wang, *Acta Pharmacol. Sin.* **2011**, *32*, 601–610.
[30] I. A. Schepetkin, L. N. Kirpotina, A. I. Khlebnikov, M. Leopoldo, E. Lucente, E. Lacivita, P. De Giorgio, M. T. Quinn, *Biochem. Pharmacol.* **2013**, *85*, 404–416.
[31] E. Lacivita, I. A. Schepetkin, M. L. Stama, L. N. Kirpotina, N. A. Colabufo, R. Perrone, A. I. Khlebnikov, M. T. Quinn, M. Leopoldo, *Bioorg. Med. Chem.* **2015**, *23*, 3913–3924.
[32] E. Lacivita, M. L. Stama, J. Maeda, M. Fujinaga, A. Hatori, M. R. Zhang, N. A. Colabufo, R. Perrone, M. Higuchi, T. Suhara, M. Leopoldo, *Chem. Biodiversity* **2016**, *13*, 875-883.
[33] M. L. Stama, J. Ślusarczyk, E. Lacivita, L. N. Kirpotina, I. A. Schepetkin, K. Chamera, C. Riganti, R. Perrone, M. T. Quinn, A. Basta-Kaim, M. Leopoldo, *J. Med. Chem.*, unpublished results.■■article submitted? DOI number? or just unpublished results?■■
[34] S. L. Skovbakke, M. Winther, M. Gabl, A. Holdfeldt, S. Linden, J. M. Wang, C. Dahlgren, H. Franzyk, H. Forsman, *Biochem. Pharmacol.* **2016**, *119*, 56–65.
[35] C. Zhou, S. Zhang, M. Nanamori, Y. Zhang, Q. Liu, N. Li, M. Sun, J. Tian, P. P. Ye, N. Cheng, R. D. Ye, M. W. Wang, *Mol. Pharmacol.* **2007**, *72*, 976–983.
[36] C. Pinilla, B. S. Edwards, J. R. Appel, T. Yates-Gibbins, M. A. Giulianotti, J. L. Medina-Franco, S. M. Young, R. G. Santos, L. A. Sklar, R. A. Houghten, *Mol. Pharmacol.* **2013**, *84*, 314–324.
[37] T. M. Stepniewski, S. Filipek, *Bioorg. Med. Chem.* **2015**, *23*, 4072–4081.
[38] P. I. Dosa, E. A. Amin, *J. Med. Chem.* **2016**, *59*, 810–840.
[39] Y.-C. Wong, Z. Ke, Y.-Y. Yeung, *Org. Lett.* **2015**, *17*, 4944–4947.
[40] E. Kelly, C. P. Bailey, G. Henderson, *Br. J. Pharmacol.* **2008**, *153*, S379–S388.
[41] R. R. Gainetdinov, R. T. Premont, L. M. Bohn, R. J. Lefkowitz, M. G. Caron, *Annu. Rev. Neurosci.* **2004**, *27*, 107–144.
[42] P. Maderna, D. C. Cottell, T. Toivonen, N. Dufton, J. Dalli, M. Perretti, C. Godson, *FASEB J.* **2010**, *24*, 4240–4249.
[43] D. Ferrari, M. Villalba, P. Chiozzi, S. Falzoni, P. Ricciardi-Castagnoli, F. Di Virgilio, *J. Immunol.* **1996**, *156*, 1531–1539.
[44] H. L. Tiffany, M. C. Lavigne, Y. H. Cui, J. M. Wang, T. L. Leto, J. L. Gao, P. M. Murphy, *J. Biol. Chem.* **2001**, *276*, 23645–23652.
[45] Y. H. Cui, Y. Le, W. Gong, P. Proost, J. Van Damme, W. J. Murphy, J. M. Wang, *J. Immunol.* **2002**, *168*, 434–442.
[46] E. A. Veal, A. M. Day, B. A. Morgan, *Mol. Cell* **2007**, *26*, 1–14.
[47] K. T. Kishida, E. Klann, *Antioxid. Redox Signaling* **2007**, *9*, 233–244.

[48] L. Zhang, G. Wang, X. Chen, X. Xue, Q. Guo, M. Liu, J. Zhao, *Sci. Rep.* **2017**, *7*, 206.
[49] K. Leuner, T. Schutt, C. Kurz, S. H. Eckert, C. Schiller, A. Occhipinti, S. Mai, M. Jendrach, G. P. Eckert, S. E. Kruse, R. D. Palmiter, U. Brandt, S. Dröse, I. Wittig, M. Willem, C. Haass, A. S. Reichert, W. E. Müller, *Antioxid. Redox Signaling* **2012**, *16*, 1421 – 1433.
[50] N. A. Colabufo, F. Berardi, M. Contino, M. Niso, C. Abate, R. Perrone, V. Tortorella, *Naunyn-Schmiedeberg's Arch. Pharmacol.* **2004**, *370*, 106 – 113.
[51] A. Azzariti, N. A. Colabufo, F. Berardi, L. Porcelli, M. Niso, M. G. Simone, R. Perrone, A. Paradiso, *Mol. Cancer Ther.* **2006**, *5*, 1807 – 1816.
[52] J. R. Hornick, J. Xu, S. Vangveravong, Z. Tu, J. B. Mitchem, D. Spitzer, P. Goedegebuure, R. H. Mach, W. G. Hawkins, *Mol. Cancer* **2010**, *9*, 298.
[53] I. Schepetkin, A. Potapov, A. Khlebnikov, E. Korotkova, A. Lukina, G. Malovichko, L. Kirpotina, M. T. Quinn, *J. Biol. Inorg. Chem.* **2006**, *11*, 499 – 513.

Manuscript received: July 20, 2017
Revised manuscript received: September 6, 2017
Accepted manuscript online: September 18, 2017
Version of record online: ■■ ■■, 0000

These are not the final page numbers! ↗↗

M. L. Stama, E. Lacivita, L. N. Kirpotina, M. Niso, R. Perrone, I. A. Schepetkin, M. T. Quinn, M. Leopoldo*

■■ – ■■

Functional *N*-Formyl Peptide Receptor 2 (FPR2) Antagonists Based on the Ureidopropanamide Scaffold Have Potential To Protect Against Inflammation-Associated Oxidative Stress

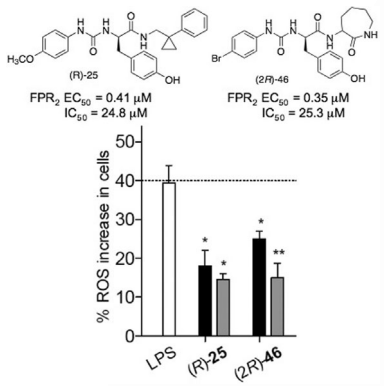

Stress relief: Prolonged oxidative stress can trigger cell death and has been implicated in the pathogenesis of many neurodegenerative diseases. We here report on a set of ureidopropanamide derivatives that behave as functional antagonists at formyl peptide receptor 2. These compounds decrease the production of reactive oxygen species in lipopolysaccharide-stimulated mouse microglial N9 cells, an in vitro model of neuroinflammation.

Lacivita & Co. @unibait @montanastate: FPR2 antagonists as potential protecting agents against #oxidative-stress SPACE RESERVED FOR IMAGE AND LINK

Share your work on social media! *ChemMedChem* has added Twitter as a means to promote your article. Twitter is an online microblogging service that enables its users to send and read text-based messages of up to 140 characters, known as "tweets". Please check the pre-written tweet in the galley proofs for accuracy. Should you or your institute have a Twitter account, please let us know the appropriate username (i.e., @accountname), and we will do our best to include this information in the tweet. This tweet will be posted to the journal's Twitter account @ChemMedChem (follow us!) upon online publication of your article, and we recommended you to repost ("retweet") it to alert other researchers about your publication.

Please check that the ORCID identifiers listed below are correct. We encourage all authors to provide an ORCID identifier for each coauthor. ORCID is a registry that provides researchers with a unique digital identifier. Some funding agencies recommend or even require the inclusion of ORCID IDs in all published articles, and authors should consult their funding agency guidelines for details. Registration is easy and free; for further information, see http://orcid.org/.

Dr. Madia L. Stama
Prof. Enza Lacivita http://orcid.org/0000-0003-2443-1174
Dr. Liliya N. Kirpotina
Dr. Mauro Niso
Prof. Roberto Perrone
Dr. Igor A. Schepetkin
Prof. Mark T. Quinn
Prof. Marcello Leopoldo

Author Contributions

M.S. Investigation: Equal; Methodology: LeadE.L. Conceptualization: Lead; Data curation: Lead; Writing – original draft: LeadL.K. Investigation: Equal; Methodology: EqualM.N. Investigation: Equal; Methodology: EqualR.P. Funding acquisition: Equal; Writing – review & editing: EqualI.S. Investigation: Equal; Methodology: Equal; Validation: EqualM.Q. Data curation: Equal; Funding acquisition: Equal; Writing – review & editing: EqualM.L. Conceptualization: Equal; Data curation: Supporting; Funding acquisition: Equal; Writing – original draft: Equal.